

Design of Dendrimer-Based Nanostructured Catalyst Systems and Their Catalytic Activity in Hydrogenation: Synthesis of Ruthenium Nanoparticles Immobilized in Dendrimer Networks

E. A. Karakhanov, A. L. Maksimov, A. V. Zolotukhina, and S. V. Kardashev

Faculty of Chemistry, Moscow State University, Moscow, 199991, Russia

e-mail: max@petrol.chem.msu.ru

Received October 27, 2009

Abstract—A new method has been proposed for immobilization of 3-nm ruthenium nanoparticles on special supports synthesized for this purpose, polymer networks based on poly(propylene imine) dendrimers. It has been shown that the structure of the support has a substantial effect on the size of particles and their catalytic activity in the hydrogenation reactions of unsaturated and aromatic compounds. The catalysts can be reused without loss of activity.

DOI: 10.1134/S0965544110040067

The use of transition metal nanoparticles in catalysis has received special attention during the last two decades. Owing to a very high specific surface area, their activity is comparable with the activity of conventional metal complex catalysts. Reactions involving these particles can be run in both homogenous and heterogeneous modes, and the catalysts are reusable. Nanoparticles of metals, such as platinum, palladium, and ruthenium, used as catalysts for hydrogenation of olefins and aromatic compounds have been shown to be the most promising [1–10].

The main problem met in the synthesis of nanoparticles and their use in catalysis is the need for their stabilization and control of their size. Aggregation during the synthesis generally leads to large particles, which are thermodynamically more stable, and, as a consequence, to a decline in catalytic activity. Basic ways of resolving the problem are the immobilization of particles in pores of heterogeneous supports [1, 2, 11] or stabilization by low-molecular-mass [5, 11–14] and macromolecular organic ligands [7–10, 15], ionic liquids [6], etc. In the majority of cases, it is necessary to find a balance between the interaction of nanoparticles with the support and their size stabilization.

We have proposed an approach to creating catalysts on the basis of nanoparticles incorporated into a crosslinked dendrimer matrix [4]. Encapsulation of nanoparticles in such materials via binding of metal ions to dendrimers (spherical symmetrical macromolecules) makes it possible to achieve a uniform distribution of particles in the bulk of the support matrix, a narrow particle-size distribution, and washout resistance. Thus, the ligand microenvironment of the catalytic site can form selectivity for a substrate [14]. The

proposed synthesis procedure includes the crosslinking of dendrimers and the subsequent encapsulation of metal nanoparticles. The catalytic activity and selectivity of these materials depend not only on the structure of dendrimer, but also on the size and rigidity of the crosslinker. The latter parameters determine to a considerable extent the size of cavities and pores of the material and, hence, the size of particles and possible diffusion constraints that emerge during the synthesis reaction.

The nanoparticles per se occur in the space between dendrimers, and the crosslinks impede their aggregation. It was shown that this approach makes it possible to fabricate effective hydrogenation catalysts on the basis of palladium nanoparticles. In this communication, we report the results of a study on the creation of ruthenium nanoparticle-based catalysts for hydrogenation of unsaturated compounds.

EXPERIMENTAL

First- and third-generation poly(propylene imine) dendrimers **DAB-PPI-G1** (**DAB(NH₂)₄**) and **DAB-PPI-G3** (**DAB(NH₂)₁₆**) were synthesized according to the procedure described in [16]. 1,6-Hexamethylene diisocyanate (HMDI) from Aldrich (98) was used as a crosslinking agent.

The IR spectra of the samples were recorded on an IR-20 spectrometer in KBr disks and on an IR-200 instrument in the attenuated total reflection mode with an HATR Multireflection accessory using a ZnSe 45° crystal for different wavelength ranges with 4-nm resolution.

Nuclear magnetic resonance analysis was performed on an Avance Bruker spectrometer operating at a frequency of 400.13 MHz. Chemical shifts were presented on the δ scale relative to TMS (δ 0.00). For aqueous solutions, 3-(trimethylsilyl)-1-propanesulfonic acid (DSS, δ 0.015) was used as a standard and D_2O and $DMSO-d_6$ were used as a solvent. The purity of the initial dendrimers was determined by mass spectrometry. The mass spectra were recorded using an Agilent LC-MS 1100 SL instrument with an electrospray ion (ESI) source in the positive-ion detection mode. The samples were prepared by dissolving in methanol (99+, Acros Organics) to have a concentration of ~10 mg/ml. The spray needle voltage was set at 3.5 kV. The temperature of the drying gas was 300°C, and the flow rate was 10 l/min.

The X-ray photoelectron spectroscopy (XPS) study of the samples was performed with a LAS-3000 instrument equipped with an OPX-150 retarding-field photoelectron analyzer. Photoelectrons were excited by X-rays from an aluminum anode ($AlK_\alpha = 1486.6$ eV) at a tube voltage of 12 kV and an emission current of 20 mA. Photoelectron peaks were calibrated by the C 1s carbon line with a binding energy of 285 eV.

Transmission electron microscopy (TEM) and electron energy loss spectroscopy (EELS) studies of the samples were performed on a LEO912 AB Omega electron microscope.

Synthesis of Catalysts

Synthesis of DAB-PPI-HMDI (1,2/1)¹. A 0.56-g portion of DAB(NH_2)₁₆ (0.33 mmol) and 120 ml of absolute THF were placed into a 250-ml flask equipped with a condenser and a magnetic stirrer. Under these conditions, the dendrimer swelled but did not dissolve. After that, 500 μ l (3.19 mmol) of hexamethylene diisocyanate was added to the flask with continuous stirring. The reaction was run at 70°C over 12 h followed by evaporation of the solvent at 50°C in a rotary evaporator. The product was obtained in the form of a milk-white powder with a yield of 1 g (91%).

IR, cm^{-1} : 3320 (N—H_{st} in NH—C(=O)); 2940 (C—H_{st}); 2855 (C—H_{st}, CH₂—N_{st}); 1770, 1620, 1570 (C=O_{st} in NH—C(=O); 1480, 1460 (N—H_d, CH_{2s}; C—N—H_d); 1440 (CH₂, δ); 1350, 1340, 1250, 1165, 1070, 1030 (C—N_{st} in NH—C(=O); 990; 735 (CH_{2y}); 640. XPS, eV: 284.9 (C 1s, 71.4%), 398.7 (N 1s, 16.3%), 530.2 (O 1s, 12.3%).

Synthesis of DAB-PPI-G1-HMDI (1,2/1). The reaction was conducted according to the same procedure. The reactants were DAB(NH_2)₄ (500 mg, 1.58 mmol) and hexamethylene diisocyanate (0.61 ml, 3.8 mmol) in 50 ml of absolute THF. The product in the form of white powder was obtained with a yield of 1 g (88%).

¹ The total NCO/NH₂ ratio was 1.2 : 1.

IR, cm^{-1} : 3310 (N—H_{st} in NH—C(=O)); 2925 (C—H_{st}); 2860 (C—H_{st}, CH₂—N_{st}); 1685, 1620, 1555 (C=O_{st} in NH—C(=O)); 1480, 1455 (CH_{2s}, C—N—H_d, N—H_d); 1370, 1335, 1255, 1210, 1175, 1040 (C—N_{st} in NH—C(=O); 990; 870 (N—H_d); 765, 725 (CH_{2y}, 625. XPS, eV: 285.4 (C 1s, 74.6%), 399.3 (N 1s, 11.6%), 530.4 (O 1s, 13.8%).

Nanoparticles were synthesized according to a modified procedure [17].

Synthesis of DAB-PPI-G3-HMDI (1,2/1)-Ru(1/8). A suspension of 200 mg of DAB-PPI-G3-HMDI(1,2/1) in 135 ml of distilled water and 100 mg (0.48 mmol) of ruthenium(III) chloride were placed into a 250-ml flask equipped with a condenser and a magnetic stirrer. The suspension rapidly turned black. The reaction was run at room temperature over 12 h. At the end of reaction, the mixture was evaporated to dryness in a rotary evaporator. The obtained powder, together with 50 ml of ethanol and 10 ml of water, was placed into a 100-ml flask with a magnetic stirrer and a condenser. Sodium borohydride in an amount of 182 mg (4.8 mmol) was added to the resulting slurry. This reaction was also conducted at room temperature over 12 h and was followed by drying in a rotary evaporator. The obtained powder was washed twice with water and ethanol and dried in air. The yield of the product (dark grey powder) was 120 mg (48%).

XPS, eV: 285.2 (C 1s, 73.1%), 398.6 (N 1s, 14.6%), 462.4 (Ru 3p_{3/2}, ≤0.5%); 531.7 (O 1s, 13.8%). UV-Vis: 9.45% Ru.

Synthesis of DAB-PPI-G1-HMDI (1,2/1)-Ru(1/4). The synthesis was performed as described above. The reactants DAB-PPI-G1-HMDI (1,2/1) (87 mg) and RuCl₃ (100 mg, 0.48 mmol) were mixed with 20 ml of water. The isolated intermediate product was suspended in a mixture of 25 ml of ethanol and 5 ml of water followed by reduction with sodium borohydride (182 mg, 4.8 mmol). The resulting black powder product was obtained with a yield of 90% (122 mg).

XPS, eV: 280.6 (Ru 3d_{5/2}); 282.2 (Ru 3d_{3/2}); 285.0 (C 1s); 399.4, 402.6 (N 1s, 16.4%); 452.2, 460.2, 461.8, 463.4 (Ru3p_{3/2}, 9.0%); 531.0 (O 1s, 74.6%). UV-Vis: 34.6% Ru.

Ruthenium in the samples was quantified spectrophotometrically with an Agilent 8453 UV/Vis instrument [17]. First, a set of 10-ml aqueous calibration solutions of RuCl₃ with concentrations of 2.2, 2.9, 4.9, and 7.5 mg/ml were prepared. Samples of DAB-PPI-HMDI(1,2/1)-Ru(1/8) (2.5 mg) and DAB-PPI-G1-HMDI(1,2/1)-Ru(1/4) (1 mg) containing ruthenium were treated with a mixture of 2 ml of concentrated HCl and 2 ml of 50% hydrogen peroxide. The resulting solutions were diluted with 6 ml of distilled water each. A 15-ml portion of 0.01 M phenanthroline solution was added to each of the calibration and sample solutions, and the solutions acquired an emerald green color. After that, 10 ml of water and 100 mg hydroxylamine hydrochloride were added to each solution and

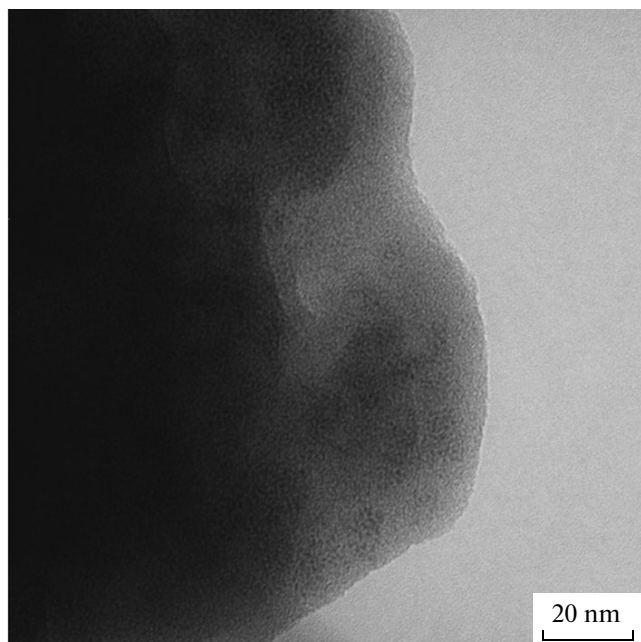


Fig. 1. Microphotograph of the DAB-PPI-G3-HMDI(1,2/1)-Ru(1/8) material.

they were heated in a water bath at 100°C for 2 h; the color gradually turned orange-red. All solutions were diluted 50-fold and spectrophotometered. The amount of ruthenium was determined by the absorbance at the 488-nm absorption band of the $[\text{Ru}(\text{phen})_3]^{2+}$ complex.

Catalyst Testing Procedure

The hydrogenation of substrates (alkylaromatic compounds) was carried out as follows. A thermostated autoclave equipped with an insert test tube and a magnetic stirrer was charged with the catalyst and a substrate taken in a ratio of 20 mg of catalyst per 1 ml of substrate. The autoclave was tightly sealed, filled with hydrogen to have a pressure of 5 atm, and connected to a thermostat. The reaction was run at 90°C over 3 h; after its completion, the autoclave was cooled down below room temperature and unsealed. The products were analyzed by gas–liquid chromatography. The substrates and the products were determined on a ChromPack CP9001 gas chromatograph with a flame-ionization detector using a 30 m × 0.2 mm column with the bonded SE-30 phase. Chromatograms were recorded and processed with the use of Maestro 1.4 software.

RESULTS AND DISCUSSION

First- and third-generation poly(propylene imine) (DAB) dendrimers were used to prepare polymer networks as supports for ruthenium nanoparticles. The crosslinking agent was 1,6-hexamethylene diisocyan-

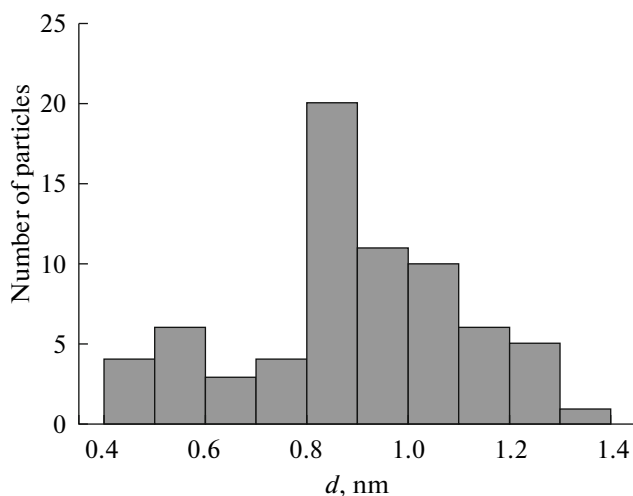


Fig. 2. DAB-PPI-G3-HMDI(1,2/1)-Ru(1/8): particle-size distribution.

ate. The reaction was conducted in a THF medium into which $\text{DAB}(\text{NH}_2)_{16}$ (or $\text{DAB}(\text{NH}_2)_4$) and $\text{OCN}(\text{CH}_2)_6\text{NCO}$ were introduced in a ratio of $\text{NCO}/\text{NH}_2 = 1.2$. The dendrimer/crosslinker ratio was chosen in such a manner as to ensure a high crosslink density of the product.

The supports (DAB-PPI-G1-HMDI (1,2/1) and DAB-PPI-G3-HMDI (1,2/1)) were obtained in a powdered form and were characterized by IR spectroscopy, X-ray photoelectron spectroscopy (XPS), and transmission electron microscopy (TEM); DAB-PPI-G3-BDI(1/3) was characterized by IR spectroscopy.

The XPS data confirmed the presence of C, N, and O atoms and the $(\text{CH}_2)_3\text{N}$, and $\text{CH}_2\text{NHC(O)NH}$ – moieties in the polymers DAB-PPI-G1-HMDI(1,2/1) and DAB-PPI-G3-HMDI(1,2/1) [18]. Signals corresponding to carbon and nitrogen were observed in the spectra. The IR spectra of the crosslinked dendrimers displayed vibrations of N–H bonds (3320 cm^{-1}), methylene groups ($2940, 2855 \text{ cm}^{-1}$), and carbonyl groups in urea fragments ($1770, 1620, 1570 \text{ cm}^{-1}$). Note that the band at $1740–1770 \text{ cm}^{-1}$ is due to cyclic urea units and the bands at 1620 and 1570 cm^{-1} are attributed to linear units. The degree of intramolecular crosslinking was defined as the ratio of peak areas at $1770, 1620$ and 1570 cm^{-1} and was estimated to be at most 6%; i.e., of every 30 isocyanate groups interacting with amino groups of different dendrimers there were two which interacted with amino groups of the same dendrimer.

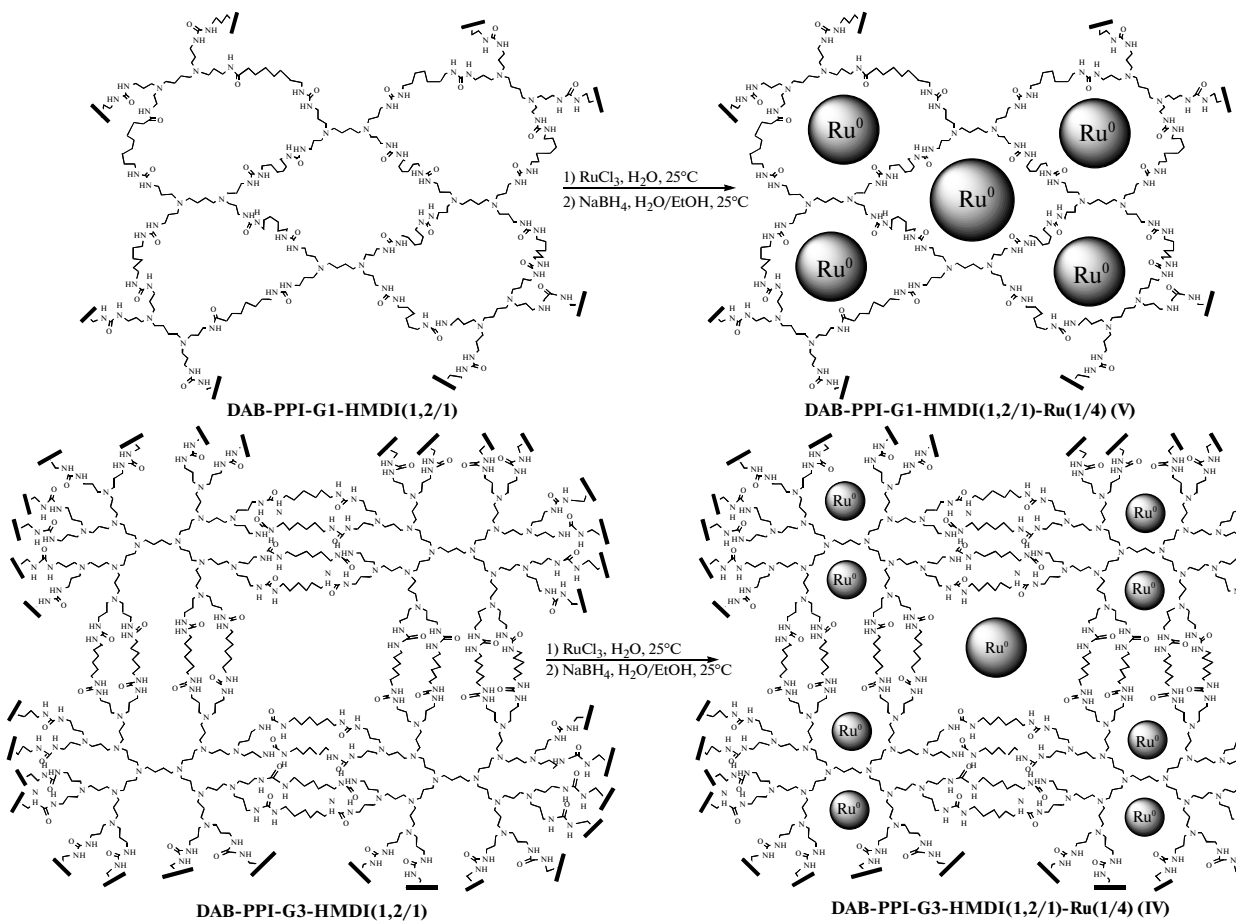
Three-dimensional models of the structural fragments of the polymer materials DAB-PPI-G1-HMDI(1,2/1) and DAB-PPI-G3-HMDI(1,2/1) are presented in Figs. 1 and 2.

At an identical crosslink density ($\text{NCO}/\text{NH}_2 = 1,2/1$), the matrix structure in the case of the first generation dendrimer (DAB-PPI-G1-HMDI(1,2/1))

has distinct cavities 2–3 nm in diameter. In contrast, such cavities are barely distinguishable in DAB-PPI-G3-HMDI(1,2/1). The TEM images (Figs. 3, 4) support our assumption on the structure of polymer materials based on crosslinked dendrimers. For example, the microphotograph of DAB-PPI-G1-HMDI(1,2/1) (Fig. 3) shows cellular fragments, which can indicate the presence of cavities in the

structure, whereas the DAB-PPI-G3-HMDI(1,2/1) sample (Fig. 4) is represented by uniform entities inside which no cavities or cells larger than 1 nm can be distinguished.

The metal nanoparticles were encapsulated in the dendrimers in two steps. Complexation with a transition metal salt was the first step, and reduction with sodium borohydride was the second step:



Hexamethylene diisocyanate-crosslinked dendrimer matrices with a high crosslink density ($\text{NCO}/\text{NH}_2 = 1,2/1$) were used to prepare ruthenium catalysts ($\text{Ru}/\text{DAB}(\text{NH}_2)_{16}$ ratios were 8 : 1 for DAB-PPI-G3-HMDI(1,2/1) and 4 : 4 for DAB-PPI-G1-HMDI(1,2/1) (V)).

It was sound that the uptake of the metal to be supported on the polymer depends on the dendrimer structure: it was 9.4 wt % for DAB-PPI-G3-HMDI(1,2/1)-Ru(1/8) or 34.6 wt % for DAB-PPI-G1-HMDI(1,2/1)-Ru(1/4). The obtained materials were characterized by XPS and TEM.

Because of overlapping with the carbon 1s line (~285 eV), the binding energies of $\text{Ru } 3p_{3/2}$, rather than those of $\text{Ru } 3d_{5/2}$ (280.6 eV) and $\text{Ru } 3d_{3/2}$ (282.2 eV), were recorded. It was shown that the metal was present in the form of both nanoparticles coordi-

nated to nitrogen atoms (462.4 eV for DAB-PPI-G3-HMDI(1,2/1)-Ru(1/8) and 461.8 eV for DAB-PPI-G1-HMDI(1,2/1)-Ru(1/4)) and the oxide RuO_2 (463.4 eV [12]) in this case. The latter peak was somewhat higher for the PPI-G1-HMDI(1,2/1)-Ru(1/4) sample, although its total height did not exceed 10%. The high oxygen content on the DAB-PPI-G1-HMDI(1,2/1)-Ru(1/4) surface can be explained in terms of rapid oxidation of ruthenium nanoparticles under the conditions of analysis [11]. The higher energy in DAB-PPI-G3-HMDI(1,2/1)-Ru(1/8) as compared to DAB-PPI-G1-HMDI(1,2/1)-Ru(1/4) is probably due to a large number of donor atoms present in the nanoparticle coordination environment (30 : 1 versus 2 : 1).

According to the TEM data, the size of particles significantly depended on the dendrimer structure, a

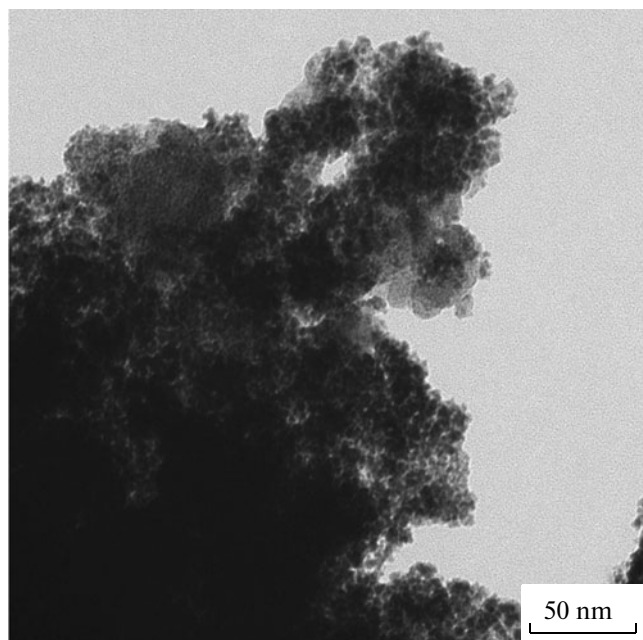


Fig. 3. Microphotograph of the DAB-PPI-G1-HMDI(1,2/1)-Ru(1/4) material.

fact that is consistent with the suggested 3D structures of the initial polymer matrices (Figs. 1, 2). For the catalysts prepared from the third-generation dendrimers,

Table 1. Hydrogenation of alkenes in the presence of ruthenium catalysts

Substrate	Time, h	Conversion, %	TOF, h^{-1}
DAB-PPI-G3-HMDI(1,2/1)-Ru(1/8)			
Hexene-1	3	46	70
Octene-1	3	38	45
Octene-1	6	92	50
Decene-1	3	4	5
DAB-PPI-G1-HMDI(1,2/1)-Ru(1/4)			
Hexene-1	1	63	75
Heptene-1	1	86	90
Octene-1	1	100	95
Nonene-1	1	29	30
Decene-1	1	27	25

Reaction conditions: 90°C, 5 atm H_2 , substrate/catalyst = 50 : 1 (by mass).

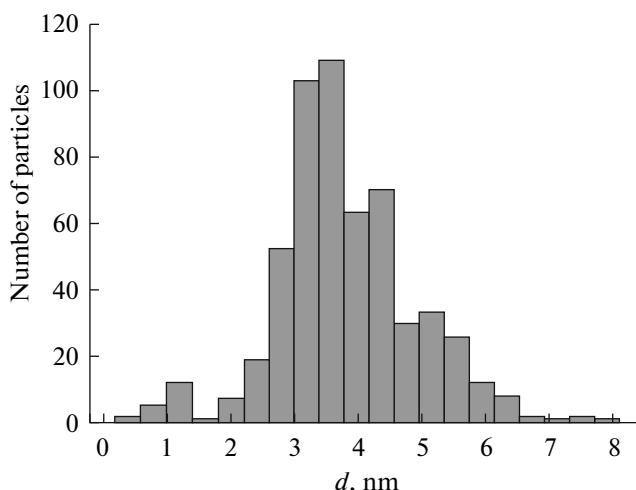


Fig. 4. DAB-PPI-G1-HMDI(1,2/1)-Ru(1/4): particle-size distribution.

the average size of nanoparticles was about 1 nm, which corresponds to the dense structure of the support (Figs. 5, 6). For the catalysts based on the first-generation dendrimers, the average particle size was about 3.5 nm, which agrees well with the cavity sizes obtained by computer simulation (Figs. 7, 8).

The materials based on ruthenium nanoparticles and hexamethylene diisocyanate-crosslinked G1 and G3 PPI dendrimers were tested in the hydrogenation reaction of terminal alkenes, conjugated systems (alkadienes and styrenes), and aromatic substrates.

It was shown that the structure of the material has a substantial effect on the activity of the catalysts in the hydrogenation of terminal olefins (Table 1). For the G3 HMDI-Ru material, which is characterized by small pores, a decrease in both the conversion and activity with an increase in the substrate chain length was observed (Figs. 9a, 9b).

The activity of DAB-PPI-G1-HMDI(1,2/1)-Ru(1/4) was significantly higher than that of DAB-PPI-G3-HMDI(1,2/1)-Ru(1/8) for hydrogenation of linear terminal olefins for all substrates except hexene-1. It increases, reaching maximum for octene-1, and sharply decreases for nonene-1, remaining relatively the same for decene. It is likely that an effect similar to that for cyclodextrin reactions [19] is observed in this case. A substrate of a smaller size, such as hexene-1, is readily adsorbed and desorbed in the support pores without additional hydrophobic interactions with the crosslink chains. In medium-sized substrates, hydrophobic interactions with these interjunction chains facilitate adsorption, thereby leading to significant acceleration of the reaction rate. For large substrates, the hydrogenation reaction occurs only on the catalyst outer surface, since the adsorption is impeded by steric hindrances.

The ruthenium catalysts based on the first- and third-generation dendrimers were also tested in the

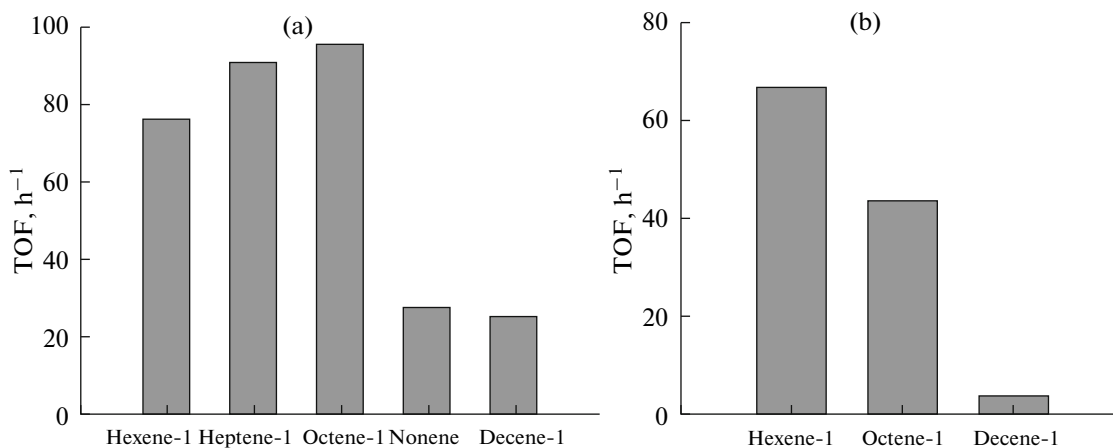


Fig. 9. Activities of the ruthenium catalysts (a) DAB-PPI-G1-HMDI(1,2/1)-Ru(1/4) and (b) DAB-PPI-G3-HMDI(1,2/1)-Ru(1/8) in the hydrogenation of terminal alkenes.

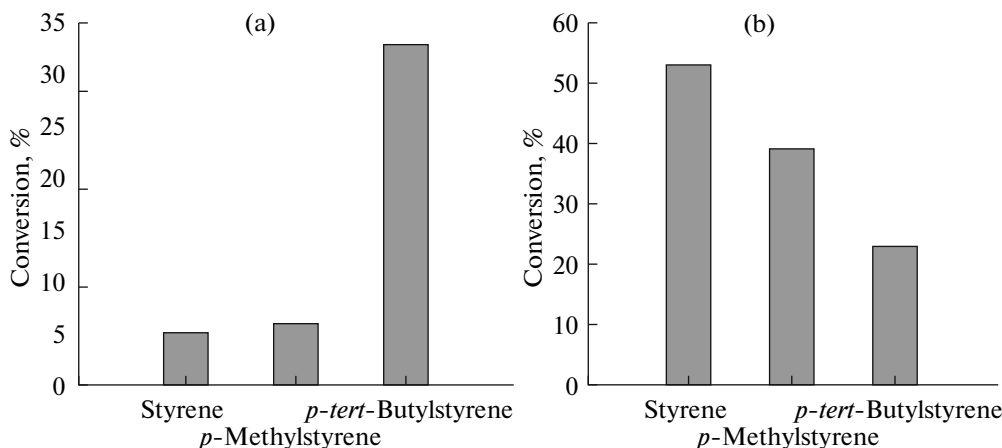


Fig. 10. Hydrogenation of styrenes in the presence of the ruthenium catalysts (a) DAB-PPI-G1-HMDI(1,2/1)-Ru(1/4) (90°C, 5 atm H_2 , 15 min, 5 mg of catalyst) and (b) DAB-PPI-G3-HMDI(1,2/1)-Ru(1/8) (90°C, 5 atm H_2 , 3 h, 5 mg of catalyst).

hydrogenation of aromatic substrates of benzene, toluene, and ethylbenzene (Table 2). The main hydrogenation products were cyclohexane derivatives formed with a selectivity of 97–100%. Even at lower conversions, no formation of the corresponding cyclohexenes in noticeable amounts was observed, a fact that can be explained by high rates of hydrogenation of these intermediates on ruthenium catalysts. Benzene was hydrogenated by 24% within 8 h over DAB-PPI-G3-HMDI-Ru and by 64% within 6 h on DAB-PPI-G1-HMDI(1,2/1)-Ru(1/4). The turnover frequency was close for both cases. Toluene was not hydrogenated in the presence of DAB-PPI-G3-HMDI-Ru, but it was still hydrogenated at a significant rate on the DAB-PPI-G1-HMDI(1,2/1)-Ru(1/4) catalyst. On passing to ethylbenzene, the rate of the reaction dramatically dropped on this catalyst as well.

Obviously, steric hindrances are already high to toluene in DAB-PPI-G3-HMDI-Ru and begin with

ethylbenzene in the case of DAB-PPI-G1-HMDI(1,2/1)-Ru(1/4). Most likely, the presence of the freely rotating alkyl group interferes with the orientation of the alkylbenzene molecule necessary for the hydrogenation reaction to occur on the surface of a nanoparticle. The effect as such depends on the pore size: the smaller the pores, the smaller the alkyl group that decreases the activity.

When the side chain of the substrate contains a double C=C bond conjugated with the benzene ring, it is this bond that is the first to be hydrogenated, with the ring itself being barely involved in the reaction. For example, quite high yields over a shorter reaction time were achieved for the hydrogenation of styrene and its derivatives as compared to benzene (Table 3).

It was shown that the conversion decreases with an increase in the size of the substrate molecule in the case of hydrogenation on DAB-PPI-G3-HMDI-Ru (Fig. 10), a trend associated with diffusion constraints

Table 2. Hydrogenation of aromatic substrates

	Substrate	T, °C	Time, h	Conversion, %
DAB-PPI-G3-HMDI(1,2/1)-Ru(1/8)				
8	Benzene	90	8	24
9	Toluene	90	8	<2
10	Benzene***	200	5	100*
	<i>o</i> -Xylene**	90	6	5*
	<i>p</i> -Xylene**	90	6	5*
	Phenol**	90	6	100*
	Anisole**	90	6	57*
DAB-PPI-G1-HMDI(1,2/1)-Ru(1/4)				
8	Benzene	90	6	64
9	Toluene	90	6	65
10	Ethylbenzene	90	6	3

Reaction conditions: 90°C, 5 atm H₂, substrate/catalyst = 50 : 1 (by mass).

Notes: * 40 atm H₂.

** A threefold increased catalyst charge.

*** A fourfold increased catalyst charge.

on the passing of the substrate through the dense dendrimer matrix. In contrast, an increase in the yield with an increase in the size of the alkyl group in the *p*-position to the vinyl group of styrene was observed in the case of DAB-PPI-G1-HMDI-Ru. We suppose that this behavior of catalytic activity can be explained by the increased contribution of hydrophobic interactions to substrate binding with an increase in the size of the substituent group.

We have hypothesized that the dendrimer-based ruthenium catalysts are characterized by an increased activity in hydrogenation of the conjugated system. To prove this assumption, we performed hydrogenation of 2,5-dimethyl-2,4-hexadiene over catalysts based on first-generation and third generation dendrimers. In the case of DAB-PPI-G1-HMDI-Ru, the conversion was 100% after 3 h, with the main product (96% selectivity) being 2,5-dimethylhexane. For DAB-PPI-G3-HMDI-Ru, the conversion over the same 3 h did not exceed 2%, of which 51% was made up of *trans*-2,5-dimethylhexene-3 and less than 40% was of 2,5-dimethylhexane. This difference in selectivity between the two catalysts seems to be caused by several factors. First, the catalytic site is more hindered in the case of DAB-PPI-G3-HMDI-Ru; as a result, it is difficult for the substrate containing isopropyl groups at the double bonds to attain the conformation in which both double bonds will be hydrogenated. Second, a large number of

Table 3. Hydrogenation of styrenes and dienes in the presence of ruthenium catalysts

Substrate	DAB-PPI-G3-HMDI(1,2/1)-Ru(1/8)			DAB-PPI-G1-HMDI(1,2/1)-Ru(1/4)		
	time, h	conversion, %	TOF, h ⁻¹	time, h	conversion, %	TOF, h ⁻¹
Styrene	3	53	85	1	5	25
<i>p</i> -Methylstyrene	3	39	55	1	6	27
<i>tert</i> -Butylstyrene	3	23	20	1	33	105
2,5-Dimethyl-2,4-hexadiene	3	2	2.5	3	100	35

Reaction conditions: 90°C, 5 atm H₂, substrate/catalyst = 50 : 1 (by mass).

nitrogen atoms per ruthenium atom (30 : 1 according to XPS data) can lower the activity of nanoparticles in the hydrogenation of monoenes because of the increase in the electron density on metal atoms [20].

In summary, the use of nanostructured systems based on crosslinked dendrimer-containing assemblies of ruthenium nanoparticles makes it possible to synthesize catalysts for hydrogenation of unsaturated compounds. Variation in dendrimer generation opens for the possibility of controlling the size of nanoparticles and their activity in hydrogenation of various substrates and affecting the selectivity of the process as in the case of molecular receptors. It is noteworthy that the obtained heterogeneous catalysts can be easily separated from the reaction products and be multiply reused without loss of activity.

ACKNOWLEDGMENTS

This work was supported by the Russian Foundation for Basic Research, project no. 07-03-00221-a, and the President of the Russian Federation under the program for encouraging young doctors of sciences, grant no. MD793.2009.3.

REFERENCES

1. J. M. Thomas, B. F. G. Johnson, R. Raja, et al., *Acc. Chem. Res.* **26**, 20 (2003).
2. M. Jacquin, D. J. Jones, J. Roziere, et al., *Appl. Catal. A: Gen.* **251**, 131 (2003).
3. F. Su, L. Lu, F. Y. Lee, et al., *J. Am. Chem. Soc.* **129**, 14213 (2007).
4. E. A. Karakhanov, A. L. Maximov, V. A. Skorkin, et al., *Pure Appl. Chem.* **81**, 2013 (2009).
5. A. Gual, M. R. Axet, K. Philippot, et al., *Chem. Commun.*, 2759 (2008).
6. M. H. G. Prechtl, M. Scariot, J. D. Scholten, et al., *Inorg. Chem.* **47**, 8995 (2008).
7. R. A. Sanchez-Delgado, N. Machalaba, and N. Ng-a-Qui, *Catal. Commun.* **8**, 2115 (2007).
8. F. Lu, J. Liu, and J. Xu, *J. Mol. Catal. A: Chem.* **271**, 6 (2007).
9. M. Ooe, M. Murata, T. Mizugaki, et al., *Nanoletters* **2**, 999 (2002).
10. N. N. Hoover, B. J. Auten, and B. D. Chandler, *J. Phys. Chem. B* **110**, 8606 (2006).
11. K. Pelzer, *Ruthenium Nanoparticles: Synthesis, Characterisation and Organisation in Alumina Membranes and Mesoporous Materials; Applications in Catalysis*. PhD Theses. (Toulouse, 2003).
12. J. Y. Lee, J. Y. Yang, T. C. Deivaraj, and H.-P. Too, *J. Colloid Interface Sci.* **268**, 77 (2003).
13. A. Nowicky, Y. Zhang, B. Leger, et al., *Chem. Commun.*, 296 (2006).
14. V. Huc and K. Pelzer, *J. Colloid Interface Sci.* **318**, 1 (2008).
15. Y. Niu and R. M. Crooks, *C. R. Chimie* **6**, 1049 (2003).
16. E.M.M. de Brabander-van den Berg and E. W. Meijer, *Angew. Chem. Int. Ed.* **32**, 1308 (1993).
17. C. V. Banks and J. W. O' Laughlin, *Anal. Chem.* **29**, 1412 (1957).
18. NIST. XPS Electronic Database. <http://srdata.nist.gov/xrs>.
19. E. Karakhanov and A. Maximov, in *Metal Complexes and Metals in Macromolecules*, Ed. by D. Wohrle and A. Pomogajlo (Wiley-VC, 2003) p. 457.
20. C. Pan, K. Pelzer, K. Philippot, et al., *J. Am. Chem. Soc.* **123**, 7584 (2001).